HHS Public Access

Author manuscript

Adv Funct Mater. Author manuscript; available in PMC 2025 November 30.

Published in final edited form as:

Adv Funct Mater. 2025 January 02; 35(1): . doi:10.1002/adfm.202410910.

Nano-Biosensors for mRNA-Based Cell Sorting Using Intracellular Markers at the Early Stage of Cell Reprogramming

Yang Song[1,2], **Jennifer Soto**[1], **Xiao Lin**[3], **Tyler Hoffman**[1], **Erin Hu**[1], **Ninghao Zhu**[4], **Jana Zarubova**[1], **Yifan Wu**[1], **Jing Tian**[1], **Pak Kin Wong**[4], **Song Li**[1,5,6,7,*]

[1]Department of Bioengineering, University of California, Los Angeles, CA 90095, USA

[2]Institute of Biomedical Engineering, West China School of Basic Medical Sciences & Forensic Medicine, Sichuan University, Chengdu 610041, China.

[3]Department of Molecular, Cell, and Developmental Biology, University of California, Los Angeles, CA 90095, USA

[4]Department of Biomedical Engineering, The Pennsylvania State University, University Park, PA 16802, USA

[5]Department of Medicine, University of California Los Angeles, Los Angeles, CA 90095, USA

[6]Eli and Edythe Broad Center of Regenerative Medicine and Stem Cell Research, University of California, Los Angeles, Los Angeles, CA 90095, USA

[7]Jonsson Comprehensive Cancer Center, David Geffen School of Medicine, University of California, Los Angeles, Los Angeles, CA 90095, USA

Abstract

Cell reprogramming and manufacturing have broad applications in tissue regeneration and disease treatment. However, many derived cell types lack unique cell surface markers for protein-based cell sorting, making it difficult to isolate these cells from mixed populations. Additionally, there is a need to identify and isolate cells of interest at the early stages of cell expansion. To address this challenge, we engineered a nucleic acid-based gold nanorod (NAGNR) fluorescent biosensor that can detect the mRNA expression of intracellular markers for cell sorting. We demonstrated its application in isolating induced neuronal (iN) cells from dermal fibroblast populations during the early stages of cell reprogramming. Cell sorting based on the mRNA of the neuronal transcriptional factor Ascl1 resulted in an enrichment of iN cells from 3% to 72%, and additional sorting with the transcriptional factor Scn2 further increased iN enrichment. Moreover, NAGNR biosensors can be used in conjunction with protein marker-based cell sorting. NAGNR-sorted iN

*Correspondence: Song Li, Ph.D. songli@ucla.edu.

Author Contributions

Y.S. and S.L. designed the experiments. Y.S., J.S., T.H., X.L., E.H., N.Z., J.Z., Y.W., and J.T. performed the experiments. Y.S., J.S., T.H., X.L., E.H., N.Z., J.Z., Y.W., and J.T. analyzed the data. Y.S., P.K.W. and S.L. contributed to data interpretation and discussion. Y.S., J.S. and S.L. wrote the manuscript.

Supporting Information

Supplementary figures and videos can be found in Supplementary Information.

Conflict of Interest Statement

The authors declare no competing interests.

cells show a functional response to electrical stimulation in a co-culture of iN cells and muscle cells. These findings demonstrate that NAGNR-based cell sorting offers great potential for cell identification and isolation at an early stage of cell reprogramming and manufacturing.

Keywords

mRNA cell sorting; gold nanorod; locked nucleic acid probes; biosensor; cell reprogramming

Introduction

Cell engineering enables the derivation of desirable cell types, offering extensive applications in regenerative medicine, disease therapy, and drug screening. For example, stem cell differentiation and cell reprogramming can be used to generate cell types such as neuronal cells, skeletal muscle cells, cardiomyocytes, and pluripotent stem cells for disease modeling or cell transplantation[1–5], and immune cell activation and expansion can be optimized to develop more robust cancer therapy[6–8]. However, for many cell types, there is no appropriate cell surface marker available for widely used fluorescence-activated cell sorting (FACS)[9]. In addition, there is a need to identify and isolate cells from mixed populations at the early stage of the cell derivation process. To address these challenges, we developed a nucleic acid-based cell sorting technology with the goal of isolating target cells at the early stage when the messenger RNA (mRNA) of phenotypic markers, including surface markers, transcriptional factors, and cytoskeletal markers, are expressed, and we also used direct cell reprogramming as a model to demonstrate the application of this technology.

As reported previously, adult mouse fibroblasts can be directly converted into induced neuronal (iN) cells via the forced expression of three transcription factors: *Ascl1*, *Brn2* and *Myt1l* (BAM)[10]. Mature and functional iN cells can be achieved in 6 weeks after BAM-transduction[11,12]. However, the reprogramming efficiency from adult fibroblasts is generally lower than 5%, and mature neurons are post-mitotic and not expandable[13]. Therefore, further isolation and purification are necessary, in addition to approaches to improve reprogramming efficiency[11,12,14]. Yet, there are two barriers to the isolation of iN cells from the fibroblast population. First, there is no appropriate cell surface markers because neuronal cells are mostly identified by transcriptional factors and cytoskeletal proteins. Secondly, most mature neuronal cells cannot survive the cell detachment and sorting processes. To overcome these barriers, there is a need to develop an approach to isolate neuronal cells at an early stage based on the expression of neuron lineage markers such as transcriptional factors. Since the fate of reprogrammed cells can be predicted at the early stage (within 2 days) due to the early lineage commitment following asymmetric cell division during iN reprogramming[15], it is possible to isolate iN cells before they become mature.

A variety of nucleotide-conjugated biosensors[16], including molecular beacons[17–20], nanoflares[21–23], nanotweezers[24] and displacement probes[25,26], have been developed to detect, temporally monitor and quantify biomolecules, such as mRNA[26,27], long coding RNAs[17] and microRNAs[28–30]. While these biosensors have provided a platform for

dynamic single cell gene expression analysis in living cells, whether these probes could be utilized for other applications, such as cell sorting, has not been explored. Here, we designed nucleic acid-based gold nanorod (NAGNR) biosensors for cell isolation based on mRNA detection[26]. The NAGNR includes locked nucleic acid fluorescent probes attached to gold nanorods (GNRs). The gold nanorod serves as a carrier of the probes into the cells via endocytosis and functions as a quencher of the fluorescent probes when they are bound to the surface of the NAGNR. The fluorescent probe includes a complementary DNA sequence for the mRNA to be detected. Upon the expression of the target mRNA in living cells, competitive binding causes the fluorescent probes to detach from the NAGNR and bind to the mRNA through the complementary sequence, making the fluorescence visible. This allows for real-time detection of the fluorescence signal and, thus, gene expression in living cells for cell identification and sorting. Therefore, the NAGNR platform provides an opportunity to sort cells based on mRNA expression, particularly in cells where surface markers are limited and thus, FACS might not be a viable option. We demonstrated that using single or multiple NAGNR biosensors, we could achieve a 10-fold enrichment of iN cells derived from dermal fibroblasts. Additionally, this technology can be combined with protein-based cell sorting for cell isolation.

Results

Optimization of NAGNR amount for live cell labeling

We first prepared a fluorophore-labeled locked nucleic acid (LNA) probe based on the PCR primer of the target gene by tagging a fluorophore at the 5′ end of the sequence (Figure 1a). The LNA probe binds with gold nanorods in Tris-EDTA buffer to generate the NAGNR. In this NAGNR biosensor, the proximity between the nanorod and the fluorophore allows effective energy transfer to quench the excited state of the fluorophore[31]. When added to cells, this fluorophore-labeled nano-sensor can be endocytosed by cells within 4 hours[26]. When the target cell expresses the lineage specific gene, the LNA binds with the mRNA sequence due to higher binding affinity and this binding reaction physically displaces the LNA from the GNR, allowing the fluorophore to emit a fluorescent signal. NAGNRs have been shown to have a higher signal-to-noise ratio to detect intracellular mRNA expression in living cells[26]. As a result, we hypothesized that FACS can be utilized to sort for fluorescently positive cells.

We then optimized the amount of GNRs to ensure sufficient fluorescence signals without compromising cell viability. Cells were subjected to varying concentrations of GNRs (from 20 to 200 μg/mL) for a duration of 6 hours, and then cell viability was examined by Live/Dead and PrestoBlue staining. Cells not cultured with GNRs served as a control. As shown in Figure 1b–c, the uptake of GNRs at concentrations exceeding 40 μg/mL induced a significant increase in cell death, which is in agreement with a previous study[26] and may be due to cytotoxicity from the accumulation of gold nanorods within the cells. Conversely, uptake of GNRs at concentrations of 20 μg/mL or 40 μg/mL did not induce any noticeable changes in cell viability (Figure 1b–c).

Subsequently, a concentration of 40 μg/mL *Ascl1*-NAGNR was utilized to detect the expression of *Ascl1* mRNA, a pioneer transcription factor essential for iN conversion

(Figure 1d)[32]. Since we noticed that NAGNRs were capable of passing through the cell nuclear membrane and entering the nucleus, we analyzed DNA damage and histone organization[33] following a 6-hour incubation of fibroblasts with GNRs (10–50 μg/mL). As shown in Figure 1e–f, GNR concentrations lower than 40 μg/mL did not induce DNA damage or histone reorganization. In addition, a GNR concentration of up to 40 μg/mL did not exhibit inhibitory effects on cell proliferation (Figure 1g).

Since iN reprogramming is a long process that can take up to 4 weeks to achieve mature neuronal cells, it is important to ensure the long-term safety of GNRs. To test for this, fibroblasts were exposed to GNRs for 6 hours and then were cultured in 1% FBS medium for a 4-week period, at which point a variety of assays were performed to assess the long-term effects of GNRs on cells (Figure 2a). To measure the intracellular GNR concentration, inductively coupled plasma mass spectrometry (ICP-MS) was utilized to detect the gold concentration within fibroblasts at different time points. As shown in Figure 2b, 7 days after fibroblasts took up the GNRs, the concentration of nanoparticles in cells decreased from 2.6 μg/sample to ~1.2 ng/sample. In addition, GNRs were not detectable by ICP-MS at 28 days after fibroblasts were exposed to the GNRs (Figure 2b). Meanwhile, cells incubated with GNRs displayed no significant difference in cell viability, DNA damage or histone H3 intensity at day 28 compared to non-GNR containing cells (Figure 2c–e). Thus, these results suggest that indeed 40 μg/mL posed no significant toxicity to cells for a long-term culture of 28 days.

While 40 μg/mL proved to be tolerable for the cells, we tested lower concentrations of the nanorods to further reduce the risk of cell damage or death. Thus, we investigated the efficacy of various concentrations of NAGNRs for cell sorting. We sought to optimize this concentration by utilizing flow cytometry to sort a target population of cells. Various concentrations (1 μg/mL to 40 μg/mL) of Texas-red modified β-actin-NAGNRs were developed to label the housekeeping gene β-actin in fibroblasts (Supplementary Figure S1). We mixed these cells with fibroblasts containing no NAGNRs in a 1:1 ratio, producing samples of cells where 50% of cells were fluorescently labeled. Flow cytometric analysis was performed to determine which concentrations of NAGNRs would be sufficient to sort out 50% of the cells. We found that at NAGNR concentrations of 10 μg/mL and above, the samples were sufficiently sorted (Figure 2f–g). Samples with NAGNR concentrations lower than 10 μg/mL displayed significantly decreased Texas-red positive cell percentages, suggesting that the sorting was not efficient (Figure 2g). Based on these findings, the GNR concentration of 10 μg/mL was chosen to be most optimal for all future experiments, in order to provide sufficient cell sorting with the lowest possible risk of cell death and DNA damage.

Sorting cells at the early phase of cell reprogramming

To investigate whether NAGNRs can be used to sort reprogrammed cells at the early stage of cell reprogramming, an ATTO488-modified endogenous *Ascl1*-NAGNR was employed to enrich iN cells at day 2 of the reprogramming process (Figure 3a). Twenty-four hours after adding doxycycline (Dox) to initiate iN reprogramming, BAM-transduced fibroblasts were incubated with *Ascl1*-NAGNR for 6 hours to label *Ascl1* mRNA in reprogrammed

cells (Figure 3b). Then, FACS was used to sort ATTO488 positive cells from the cell population, and we found that more than 90% of the sorted cells were Ascl1$^+$ cells (Figure 3c and Supplementary Figure S2). The sorted cells were then further cultured in neuronal medium to allow for iN cell maturation. To quantify the enrichment of iN cells, mRNA quantification and immunostaining of neuron-specific markers were performed on days 7, 14, and 28. Quantification of relative mRNA expression on day 2 showed that sorted cells displayed significantly higher expression of *Ascl1*, a gene encoding for the proneural transcription factor, as compared to non-sorted cells (Figure 3d). Simultaneously, we found that the mRNA expression of neuron-specific β-tubulin-encoding gene *Tubb3* increased significantly as compared to non-sorted cells (Figure 3d). On day 4 and day 7, there was a significantly higher proportion of Tau$^+$ and Tubb3$^+$ cells, which are early neuronal markers, in the sorted cell populations as compared to the non-sorted cells (Figure 3e–f). After four weeks, immunostaining was performed to analyze the expression of mature neuronal marker, microtubule associated protein 2 (MAP2), in sorted and non-sorted cells. We found that iN cells from both sorted and non-sorted populations expressed MAP2, with a larger proportion of MAP2$^+$ cells in the sorted cells (Figure 3g and Supplementary Figure S3). Furthermore, analyzing iN cell viability via a Prestoblue assay or quantifying the percentage of live Tau-GFP$^+$ iN cells showed that GNRs did not affect iN cell viability after 1 week, suggesting that the iN cells were viable (Supplementary Figure S4). Similarly, iN cells retained functionality at 6 weeks after exposure to GNRs (Supplementary Video 1). Taken together, these results indicate that cell sorting using NAGNRs can efficiently enrich the reprogrammed cells at the early stage of cell reprogramming.

Sorting cells using two mRNA markers

We also explored the use of multiple mRNA markers to sort cells, and investigated the ability to sort for two separate early neuronal markers, *Ascl1* and *Scn2*. *Scn2* is a gene that is highly expressed in excitatory neurons, and can be expressed within 36 hours after iN reprogramming induction[15]. Typically, *Ascl1* is upregulated immediately after reprogramming, while *Scn2* tends to be upregulated just as *Ascl1* is downregulated[15]. Based on the temporal relationship of these genes, we hypothesized that if we could sort for *Ascl1*$^+$ and *Scn2*$^+$ cells sequentially then we might obtain a population of specific type of neurons.

To test for this possibility, a NAGNR double sorting was performed to purify reprogrammed iN cells during the first 72 hours of cell reprogramming by FACS, after first confirming that multiple GNR treatments did not affect cell viability (Supplementary Figure S5). As shown in Figure 4a, ATTO488-modified endogenous *Ascl1*-NAGNRs and Cy5-modified endogenous *Scn2*-NAGNRs were prepared to label reprogrammed cells expressing *Ascl1*, *Scn2* or both. Due to the temporal kinetics of *Ascl1* and *Scn2* expression during iN reprogramming, sequential sorting was processed based on *Ascl1* first, followed by *Scn2*. On day 2, cells were sorted for *Ascl1*, and the population of sorted cells were placed back into culture (Figure 4b and Supplementary Figure S6). Then, 24 hours later, the sorted cell population was again sorted using *Scn2*-NAGNRs (Figure 4c and Supplementary Figure S6). Quantitative polymerase chain reaction (qPCR) analysis was performed to analyze *Tubb3* gene expression in the non-sorted, single-sorted (*Ascl1*$^+$), and double-sorted (*Ascl1*$^+$ and

Scn2$^+$) populations after 4 days. As expected, the expression of *Tubb3* increased in single-sorted populations relative to non-sorted, and even further increased from single-sorted to double-sorted (Figure 4d). In addition, consistent with these results, the double-sorting further enriched Tubb3$^+$ cells at day 7 (Figure 4e–f), improving the iN yield from 69% to 79% when compared to single marker sorting (Supplementary Figure S7). Similarly, double marker sorting enhanced the proportion of MAP2$^+$ cells at day 28 (Figure 4g and Supplementary Figure S8). These results suggest that various NAGNRs can be used to continuously sort target cells by labeling different mRNA markers at different stages of cell reprogramming to attain a population of specific neurons.

Sorting cells by using mRNA and protein markers

Furthermore, we sought out to investigate whether NAGNRs can be combined with a cell surface marker to sort target cells. For these experiments, embryonic stem cells (ESCs) were cultured in endothelial cell induction medium mixed with N2B27 neuronal induction medium (1:1 ratio) for 10 days to simultaneously induce ESC differentiation into endothelial and neuronal cells. The differentiated ESC populations were then labeled with PE-conjugated CD105 antibody and ATTO488-modified *Ascl1*-NAGNRs for 6 hours (Figure 4h and Supplementary Figure S9). FACS was employed to sort for PE$^+$ cells and ATOO488$^+$ cells at the same time (Figure 4i and Supplementary Figure S10). After cell sorting, the sorted PE$^+$ cells were cultured in endothelial cell medium for 1 week, and immunofluorescence analysis showed that the PE sorted cells were indeed endothelial cells as they expressed CD31 on the cell surface (Figure 4j). Concurrently, culturing the sorted ATOO488$^+$ cells in neuronal media for one week revealed that these cells highly expressed Tubb3, indicating that they had differentiated into neuronal cells (Figure 4k). In addition, ATTO488-modified *Ascl1*-NAGNRs could be combined with an RFP-conjugated CD68 antibody to purify iN cells from macrophages during macrophage-mediated iN reprogramming (Supplementary Figure S11). These results support the ability of NAGNR-aided sorting to be combined with traditional protein-based cell sorting, thereby potentially enhancing the cell purification process.

Using purified iN cells in an in vitro neuromuscular co-culture model

The ability to derive a large number of purified iN cells will enable patient-specific neuronal disease modeling or regenerative therapies. To demonstrate this potential, we conducted experiments testing the integration of iN cells with muscle cells for the study of neuromuscular interactions *in vitro*. In these experiments, iN spheroids were cultured on a single layer of fused myotubes, and electrical stimulation was applied to the culture (Figure 5a). Confirming the increased success of reprogramming via NAGNR-aided sorting, the expression of Tau was increased in spheroids containing sorted iN cells relative to spheroids with un-sorted iN cells (Figure 5b). Following 8 days of co-culture, we recorded videos of cellular contractions with and without electrical stimulation to determine the influence of iN spheroids on functional contraction output. Using Myocyter to extract parameters related to contraction from whole frame videos, we determined the magnitude of contractions over time and amplitude for each detected contraction. We first identified that C2C12 cells cultured in the absence of neuronal spheroids had limited contractions in the presence of electrical stimulation, based on minimal fluctuations in contraction

magnitude over time (Supplementary Figure S12). C2C12 myotubes in the presence of control (non-sorted) iN spheroids demonstrated more spontaneous contractions that increased when stimulation was applied. Compared to the control iN spheroids, sorted iN spheroids led to limited spontaneous contractions in the absence of stimulation, but more robust fluctuations of contractions over time when stimulation was applied (Figure 5c). The contractions of sorted iN spheroid co-cultured with myotubes appeared more periodic and less noisy compared to that of control iN spheroids. This may be due to the fact that control iN spheroids were not as compact as sorted spheroids, tended to disaggregate, and spread over more surface area. This could potentially explain the observed increased contraction amplitude, as the quantification of contraction parameters is measured based on overall displacement of myotube monolayers. We noticed this led to more desynced contractions across the whole frame for the control group, whereas the compact sorted spheroids demonstrated more localized inducible contraction in the proximity of the iN spheroid (Supplementary Figure S13, Supplementary Video 2). The presence of control or sorted iN spheroids without stimulation demonstrated higher amplitudes of contractions, compared to C2C12 only cultures with stimulation (Figure 5d). Interestingly, sorted iN spheroids led to a statistically significant increase in mean contraction amplitude during stimulation, compared to that of no stimulation (Figure 5d). Control spheroids did not show a significant change in contraction amplitude in the presence or absence of stimulation due to a wide variation of responses. This may be due to low number of iN cells in the unsorted spheroids, which reduces the frequency of neuromuscular junction formation and caused inconsistent responses. Moreover, we evaluated parameters of minimum, maximum and mean contraction, and number of beats (fold change of stimulation group compared to no stimulation) between contraction amplitudes in Figure 5e. Sorted iN spheroids outperform control spheroids in all parameters after normalizing to non-stimulated conditions, indicating a more suitable platform for investigating electrical stimulation-induced myogenic contractions via neuromuscular junctions.

Discussion

Here, we show for the first time, that a NAGNR biosensor can be utilized to sort cells during cell reprogramming based on mRNA expression, contributing to cell sorting techniques and demonstrating a new application for nucleotide-conjugated biosensors (Figure 5f). By designing complementary nucleic acid probes for mRNAs of neuronal markers (Ascl1, Scn2) and identifying an optimal level of NAGNRs that did produce any side effects on cell viability and functions, we were able to isolate iN cells from dermal fibroblast populations in a highly efficient manner, improving the iN cell yield from 3% to 70%. Through the application of multiple NAGNR biosensors, we found that we could further enrich for desired target cells, resulting in an iN cell yield of 80%. With an isolation efficacy greater than 85%, this NAGNR platform is capable of sorting cells in a manner that is comparable to conventional cell isolation strategies, such as surface marker-based cell sorting. Moreover, we showed that NAGNR biosensors could be used in conjunction with protein marker-based cell sorting, allowing for successful isolation of two distinct cell types in an ESC differentiation model. The isolated cells remained viable and functional after sorting, demonstrating the potential of this cell sorting technology for downstream

biomedical applications. Indeed, based on our findings, this sorted technology could potentially be utilized to generate patient-derived disease models, such as neuromuscular junctions to evaluate drug candidates that could improve muscle function. We found that sorted spheroids showed a higher extent of inducible contractions, possibly providing a more reliable model for neuromuscular junction function by detecting changes in stimulated contractions in the presence of various drug candidates.

A significant advantage of this mRNA-based cell sorting approach is its ability to identify and isolate desirable cell types at early stages of cell reprogramming, differentiation, or activation. Isolating these cells early provides several benefits. First, certain cell types, such as neurons and cardiomyocytes, may not survive traditional isolation procedures once they reach more mature stages. Secondly, early enrichment of specific cell populations is often essential for processes like cell manufacturing, including chimeric antigen receptor (CAR)-T cell expansion. This enables the targeted isolation of activated subpopulations, enhancing the effectiveness of immunotherapies. Thirdly, mRNA-based sorting facilitates the isolation of cells soon after gene editing or gene introduction, helping to overcome challenges such as low efficiency and supporting further cell expansion. Therefore, by capturing cells at these early stages, this approach optimizes both cell survival and scalability for downstream applications.Current neuron isolation technologies rely on intracellular staining, genetically labeled cells, fresh cells/tissue, or fluorescently labeled transporter ligands, and may not be compatible with downstream biochemical analyses after processing[34–38]. In some cases, neurons are isolated nonspecifically by removing non-neuronal cells from the culture using antibodies and magnetic-based cell sorting[39] or depend on isolating neural progenitor cells using a cell adhesion marker from which neurons can be derived from[40]. On the other hand, the NAGNR biosensor provides an opportunity to isolate neuronal cells based on mRNA expression, therefore not reliant on genetically labeled cells to separate different neuronal subtypes. This platform does not require transfection and minimizes perturbation to the cells, providing a noninvasive method to isolate cells that allows for downstream molecular analysis (e.g. qPCR and immunostaining). However, the NAGNR platform depends on internalization of the GNR-LNA complexes via endocytosis and thus, it is limited to living cells[26]. While it is possible to isolate neurons from fixed tissue utilizing FACS[36], these still require mincing tissues and staining for intracellular markers, which is only suitable for cell type analysis but not for functional studies or isolating cells for disease modeling or therapy

Although we applied this tool to isolate target cells (i.e. iN and endothelial cells) mainly during cell reprogramming and differentiation, it could also be utilized to purify a wide range of source cells, including rare cells within a population, and can be combined with other gene-level and protein-level sorting methods to attain pure cell populations, demonstrating the versatility of this platform. In addition, the ability to sort cells using distinct NAGNRs that recognize specific target genes provides the possibility to sort for different cell types in mixed cell populations or at different time points during cell reprogramming, depending on the gene expression within the cells at any given time point. Thus, it may be possible to isolate different cellular subtypes, in particular post-mitotic cells, during such processes, providing an opportunity to obtain purified cultures for cell therapy, tissue engineering or genomic analysis[41–43]. Moreover, although we showed

that NAGNR biosensor can be utilized to sort cells by FACS, whether other nucleotide-conjugated biosensors can be applied for cell sorting remains to further explored. However, it is important to mention that this isolation strategy is highly dependent on the timely expression of particular mRNA within target cells, the binding efficacy of the probe, and the expression of fluorescence after mRNA binding. Fluctuations in any of these variables could potentially affect the cell sorting process and limit the types of cells that can be isolated. Despite these limitations, this NAGNR-based cell sorting is a promising platform for cell isolation and purification that may be highly valuable for regenerative medicine.

Methods

All experiments were performed in accordance with relevant guidelines and ethical regulations approved by the UCLA Institutional Biosafety Committee (BUA-2016-222).

Cell isolation, culture and reprogramming

Mice utilized in these studies were housed under specific pathogen-free conditions and 12-hour light/12-hour dark cycles with controlled temperature and humidity settings, as previously described[11]. All experiments were performed in accordance with relevant guidelines and ethical regulations approved by the UCLA Institutional Animal Care and Use Committee (Protocol # ARC-2016-036 and ARC-2016-101).

Fibroblasts isolated from ear tissues of 1 month-old adult C57BL/6 mice (Jackson Laboratory, 002052) and Tau-EGFP reporter mice (Jackson Laboratory, 004779) were expanded in fibroblast medium: DMEM (Gibco, 11965), 10% fetal bovine serum (FBS; Gibco, 26140079) and 1% penicillin/streptomycin (Gibco, 15140122). For reprogramming experiments, fibroblasts were synchronized upon reaching 80% confluency using DMEM with 1% FBS for 24 hours before transduction with BAM-containing viruses, as described previously [11]. The following day (day 0), the medium was changed to mouse embryonic fibroblast (MEF) medium containing doxycycline (2 ng/ml, Sigma) to initiate the reprogramming process. The next day (day 1), cells were cultured in N2B27 medium: DMEM/F12 (Gibco, 11320033), N-2 supplement (Gibco, 17502048), B-27 supplement (Gibco, 17504044), 1% penicillin/streptomycin, and doxycycline (2 ng/ml), and half medium changes were performed every 2 days. On day 7, cells were fixed and stained for neuronal beta-tubulin III (Tubb3) to determine the reprogramming efficiency, which was defined as the percentage of iN cells on day 7 relative to the number of the cells initially seeded. To assess the maturation and functionality of the iN cells, cells were kept in culture for the indicated time points (i.e. 4–6 weeks). Reprogramming of iN cells from macrophages was performed as previously described [11].

Lentiviral preparation and transduction

Fibroblasts were transduced with doxycycline-inducible lentiviral vectors for Tet-O-FUW-Brn2, Tet-O-FUW-Ascl1, Tet-O-FUW-Myt1l, and FUW-rtTA plasmids to induce the expression of Brn2, Ascl1, Myt1L, and rtTA, as reported previously[11,12,14]. Lentivirus produced by using established calcium phosphate transfection methods was concentrated using Lenti-X Concentrator (Clontech, 631232) according to the manufacturer's protocol.

Synchronized fibroblasts were transduced with BAM constructs in the presence of polybrene (8 μg/ml; Sigma, H9268) for 24 hours prior to performing NAGNR cell sorting experiments.

NAGNR labeling and GNR concentration

To detect mRNA expression in living cells for cell sorting, we first prepared a fluorophore-labeled locked nucleic acid (LNA) probe based on the PCR primer of the target gene by tagging a fluorophore at the 5′ end of the sequence, and resuspended the probe at 100 μM in 1x Tris-EDTA buffer, as described previously [26]. The LNA was combined with the gold nanorods in Tris-EDTA buffer to generate the NAGNR biosensor. The gold nanorod (GNR) (Nanopartz, C12-10-1064-TMU-DIH-50-1) was 10 nm in diameter, 67 nm in length, with an SPR of 1064 nm, and was modified with mercaptoundecyltrimethylammonium bromide (MUTAB). To detect mRNA expression for iN cell sorting, BAM-transduced fibroblasts treated with doxcycline for 24 hours were collected and plated in a 24 well plate at 10,000 cells/well, and NAGNR complexes specific to *Ascl1* and/or *Scn2* were added to the culture media as described previously[26]. Briefly, NAGNR complexes were made by mixing 1.5 μl LNA Probe (10 μM), 2.5 μl GNR (Nanopartz, C12-10-1064-TMU-DIH-50-1) and 46 μl Tris-EDTA buffer, and incubating at 37°C for 15 minutes. The NAGNR complex solution (50 μl) and fresh culture medium (450 μl) were then mixed and added to the cells. After 6-hour incubation, cells were washed with PBS, and fresh culture medium was added. Cells were incubated at 37 °C in the dark for an additional 60 minutes prior to performing live cell imaging. To detect the GNR concentration, cells were incubated with GNRs for 6 hours and washed 3x with PBS. 10×10^6 cells were collected at the indicated time points and freeze dried for 2 days. Then the gold concentration in cells was detected by Inductively Coupled Plasma Mass Spectrometry (ICP-MS), where μg refers to the amount of gold nanorods in 10×10^6 cells.

Cell viability assays

After cells were cultured with GNRs for 6 hours, 1×10^4 fibroblasts were plated and allowed to attach for 24 hours in a 96 well plate. To assess cell viability, the LIVE/DEAD™ Cell Imaging Kit (Invitrogen, R37601) was implemented according to the manufacturer's protocol and as reported previously[11]. Epifluorescence images were collected using a Zeiss Axio Observer Z1 inverted fluorescence microscope and analyzed using ImageJ.

Cell viability was also evaluated using the PrestoBlue® Cell Viability Reagent (Invitrogen, A13261) according to the manufacturer's protocol and as described previously[14]. After incubating cells with the PrestoBlue Reagent for 2 hours, absorbance was measured using a plate reader (Infinite 200PRO) at excitation/emission= 560/590 nm. Results were normalized to control samples (i.e., cells cultured with no GNR).

DNA damage assays

After cells were cultured with GNRs for 6 hours, 5×10^3 fibroblasts were plated and allowed to attach for 12 hours in a 96 well plate. To assess DNA damage, the HCS DNA Damage Kit (Invitrogen, H10292) was implemented according to the manufacturer's protocol and as described previously[11]. Epifluorescence images were collected using a Zeiss Axio

Observer Z1 inverted fluorescence microscope and analyzed using ImageJ. Results were normalized to control samples (i.e., cells not treated with GNRs).

Immunofluorescence staining, imaging, and quantification

Samples collected for immunofluorescence staining at the indicated time points were washed once with PBS, fixed in 4% paraformaldehyde for 15 minutes and immunostained as described previously[11]. Samples were permeabilized using 0.5% Triton X-100 for 10 minutes and blocked with 5% normal donkey serum (NDS; Jackson Immunoresearch, 017000121) in PBS for 1 hour. Samples were incubated with primary antibodies [Tuj1/Tubb3 (Biolegend, 801202; 1:1000), MAP2 (Biolegend, 801801; 1:200), CD31 (Biolegend, 160207; 1:50)] in antibody dilution buffer (1% normal donkey serum (NDS) + 0.1% Triton X-100 in PBS) for 1 hour at room temperature followed by three PBS washes and a 1-hour incubation with Alexa Fluor secondary antibodies [Donkey anti-Mouse IgG (H+L) Highly Cross-Adsorbed Secondary Antibody, Alexa Fluor™ 546 (ThermoFisher, A-10036), Donkey anti-Rabbit IgG (H+L) Highly Cross-Adsorbed Secondary Antibody, Alexa Fluor™ 546 (ThermoFisher, A-10040)], and/or Donkey anti-Mouse IgG (H+L) Highly Cross-Adsorbed Secondary Antibody, Alexa Fluor™ 488 (ThermoFisher, A-21202)] and 4’,6-diamino-2-phenylindole (DAPI; ThermoFisher, D3571) in PBS to label the nuclei. Epifluorescence images were collected using a Zeiss Axio Observer Z1 inverted fluorescence microscope and analyzed using ImageJ.

Average histone H3 intensities per nuclei were quantified using an ImageJ macro, as described previously[11]. To create individual selections for each nucleus, Gaussian blur, thresholding, watershed, and analyze particle functions were applied to the DAPI channel. This mask was then applied to the corresponding stain image to determine the average fluorescence intensity within each nucleus.

EdU labeling and staining

EdU labeling and staining was performed using the Click-iT EdU Alexa Fluor 488 Imaging Kit (ThermoFisher, C10337) according to the manufacturer’s protocol and as reported previously[15]. Briefly, BAM-transduced fibroblasts incubated with 10 μM EdU for 3 hours were fixed with 4% paraformaldehyde (Electron Microscopy Sciences, 15710) for 15 minutes at room temperature, followed by three washes with 3% bovine serum albumin (BSA; Fisher, BP1600) in phosphate-buffered saline (PBS). Samples were then permeabilized with 0.5% Triton X-100 (Sigma, T8787) in PBS for 20 minutes, washed twice with 3% BSA in PBS and incubated with the EdU cocktail reaction for 30 minutes. Samples were washed twice with 3% BSA in PBS and stained with DAPI for 10 minutes to identify nuclei.

Fluorescence Activated Cell Sorting and Flow cytometry analysis

After adding Dox to initiate iN reprogramming, NAGNR complexes specific to *Ascl1* and *Scn2* were added to culture media for 6 hours to label *Ascl1* and *Scn2* gene expression in BAM-transduced fibroblasts at day 1 and day 2, respectively. The cells were washed with PBS 3 times and incubated in N2B27 neuronal induction medium for 24 hours. *Ascl1* and *Scn2*-mRNA labeled fibroblasts were then collected in cold FACS buffer and sorted using a

BD FACSAria II or BD FACSAria III Cell Sorter. After cell sorting, cells were seeded in a 24 well plate coated with fibronectin and cultured in N2B27 medium for 7 days, at which point cells were fixed and stained for Tubb3 to determine the iN reprogramming efficiency. For endothelial cell sorting after ESC differentiation into endothelial cells for 10 days, cells were incubated with a PE conjugated CD105 antibody (Biolegend, 120407; 1:200)] diluted in FACS buffer for 1 hour at room temperature to label the cell surface marker. The cells were washed 3 times with PBS and collected in FACS buffer for cell sorting. After sorting, CD105 positive cells were cultured in endothelial medium for 10 days, and samples were fixed and stained for CD31 staining to identify the endothelial cells. For flow cytometry experiments, sample acquisition was conducted using the Attune NxT digital flow cytometer (ThermoFisher Scientific) and the data were analyzed using FlowJo v10 software.

Reverse transcription and quantitative polymerase chain reaction (RT-qPCR)

Sorted and non-sorted cells were plated in 60-mm dishes and at the indicated time points, samples were lysed using TRIzol™ Reagent (Invitrogen, 15596026), and RNA was isolated as described previously[11,14]. Upon extracting the RNA, first-strand cDNA synthesis was prepared using the ThermoScientific Maxima First Strand cDNA Synthesis Kit (ThermoFisher, K1641). qRT-PCR was then performed using a CFX96 Real-Time PCR Detection System to detect the mRNA levels of endogenous *Ascl1* (Forward primer: CAACCGGGTCAAGTTGGTCA, Reverse primer: CTCATCTTCTTGTTGGCCGC), and *Tubb3* (Forward primer: GCGCCTTTGGACACCTATTC, Reverse primer: CACCACTCTGACCAAAGATAAAGTTGT), where *18S* (Forward primer: GCCGCTAGAGGTGAAATTCTTG, Reverse primer: CATTCTTGGCAAATGCTTTCG) was used for normalization.

iN cell and muscle co-culture and electrophysiological measurements

C2C12 (ATCC, CCRL-1772) were seeded at 5.3×10^4 / cm^2 in a 24-well plate and incubated in DMEM+10%FBS+1%P/S for 48 hours. Cultures were then changed into myogenic induction media (DMEM+2% Horse Serum) for 5 days to promote fusion. Media was changed every 2 days. Unsorted and sorted neural spheroids were created using an AggreWell 400 (StemCell Technologies, 34415). Following day, unsorted and sorted neural spheroids were resuspended in neuronal induction media and added to the myogenic cultures. Final media formulation included 1:1 ratio of neuronal to myogenic medium. Co-cultures were maintained for 8 additional days prior to stimulation measurements. Briefly, co-cultured cells were connected to a square pulse stimulator (Grass Astro-Med, S88X) using two needle electrodes (MFI Medical, TE/S50716–001). During imaging, the stimulator generated a monophasic repeating pulse wave with a duration of 0.005 seconds at a frequency of 1 Hz. The output voltage was adjusted based on the volume of the culture medium, with 15V of electrical stimulation applied per 1 ml of culture medium. Videos of myotube contractions were taken in the presence or absence of stimulation (45V) for 15 seconds. The same location was recorded without and with stimulation. Quantifications were performed on ImageJ using Myocyter[44] v1.5 to extract parameters of contraction intensity across the whole frame (Threshold 0, Detection 10) and identify amplitude peaks.

Statistical analysis

All data are presented as mean ± one standard deviation (SD). Box plots show the ends at the quartiles, the mean as a horizontal line in the box, and the whiskers represent the SD. For all experiments, the sample size n was at least 3 ($n \geq 3$) replicates unless otherwise specified. When sample size indicates a certain number of cells were examined, these results were obtained from analyzing cells across 3 samples. For two group analysis, a two-tailed, unpaired Student's *t*-test was used to analyze differences. For comparisons among values for groups greater than two, a one-way analysis of variance (ANOVA) followed by a Tukey's post-hoc test was performed. For all cases, we set significance level $\alpha=0.05$ with a 95% confidence to detect a significant difference, and p-values less than 0.05 were considered statistically significant. Origin 2018 software was used for all statistical evaluations.

Supplementary Material

Refer to Web version on PubMed Central for supplementary material.

Acknowledgements

The authors were supported in part by innovation grants from Eli and Edythe Broad Center of Stem Cell Research, the Jonsson Comprehensive Cancer Center, and California NanoSystems Institute at UCLA, and grants from the National Institute of Health (GM143485, NS130677 and NS126918 to S.L.). The authors acknowledge the use of instruments at the Advanced Light Microscopy and Spectroscopy Lab at the California NanoSystems Institute, the UCLA Flow Cytometry Core facility and the Nano and Pico Characterization Laboratory at CNSI. The content is solely the responsibility of the authors and does not necessarily represent the official views of the National Institutes of Health.

Data Availability

The authors declare that all data supporting the findings of this study are available within the paper and supplementary information files.

References

[1]. Wang H, Yang Y, Liu J, Qian L, Nat. Rev. Mol. Cell Biol 2021, 22, 410. [PubMed: 33619373]

[2]. Bocchi R, Masserdotti G, Götz M, Neuron 2022, 110, 366. [PubMed: 34921778]

[3]. Fang J, Sia J, Soto J, Wang P, Li LAK, Hsueh YY, Sun R, Faull KF, Tidball JG, Li S, Nat. Biomed. Eng. 2021 58 2021, 5, 864.

[4]. Downing TL, Soto J, Morez C, Houssin T, Fritz A, Yuan F, Chu J, Patel S, V Schaffer D, Li S, Nat. Mater 2013, 12, 1154. [PubMed: 24141451]

[5]. Song Y, Soto J, Chen B, Yang L, Li S, Biomaterials 2020, 234, 119743. [PubMed: 31962231]

[6]. Chen LC, Chen YY, Curr. Opin. Biotechnol 2019, 60, 111. [PubMed: 30822698]

[7]. Li YR, Wilson M, Yang L, Front. Immunol 2022, 13, 999549. [PubMed: 36275727]

[8]. Liu Z, Li Y, Angeles L, Yang Y, Zhu Y, Yuan W, Hoffman T, Angeles L, Wu Y, Angeles L, Zhu Y, Fang Y, Ge X, Soto J, Angeles L, Yang L, Angeles L, Preprint 2023, 1.

[9]. Robinson JP, Ostafe R, Iyengar SN, Rajwa B, Fischer R, Cells 2023, 12, DOI 10.3390/CELLS12141875.

[10]. Vierbuchen T, Ostermeier A, Pang ZP, Kokubu Y, Südhof TC, Wernig M, Nature 2010, 463, 1035. [PubMed: 20107439]

[11]. Song Y, Soto J, Chen B, Hoffman T, Zhao W, Zhu N, Peng Q, Liu L, Ly C, Wong PK, Wang Y, Rowat AC, Kurdistani SK, Li S, Nat. Mater 2022, 21, 1191. [PubMed: 35927431]

[12]. Soto J, Song Y, Wu Y, Chen B, Park H, Akhtar N, Wang P, Hoffman T, Ly C, Sia J, Wong S, Kelkhoff DO, Chu J, Poo M, Downing TL, Rowat AC, Li S, Adv. Sci 2023, 10, 2300152.

[13]. Aranda-Anzaldo A, Commun. Integr. Biol 2012, 5, 134. [PubMed: 22808316]

[14]. Song Y, Soto J, Wong SY, Wu Y, Hoffman T, Akhtar N, Norris S, Chu J, Park H, Kelkhoff DO, Ang CE, Wernig M, Kasko A, Downing TL, Poo MM, Li S, Sci. Adv 2024, 10, 639.

[15]. Song Y, Soto J, Wang P, An Q, Zhang X, Hong SG, Lee LP, Fan G, Yang L, Li S, Adv. Sci 2021, 8, DOI 10.1002/advs.202003516.

[16]. Zhou Q, Son K, Liu Y, Revzin A, Annu. Rev. Biomed. Eng 2015, 17, 165. [PubMed: 26274599]

[17]. Kam Y, Rubinstein A, Naik S, Djavsarov I, Halle D, Ariel I, Gure AO, Stojadinovic A, Pan HG, Tsivin V, Nissan A, Yavin E, Cancer Lett 2014, 352, 90. [PubMed: 23416875]

[18]. Chen M, Ma Z, Wu X, Mao S, Yang Y, Tan J, Krueger CJ, Chen AK, Sci. Reports 2017 71 2017, 7, 1.

[19]. Tyagi S, Nat. Methods 2009 65 2009, 6, 331.

[20]. Mao S, Ying Y, Wu R, Chen AK, iScience 2020, 23, 101801. [PubMed: 33299972]

[21]. Seferos DS, Giljohann DA, Hill HD, Prigodich AE, Mirkin CA, J. Am. Chem. Soc 2007, 129, 15477. [PubMed: 18034495]

[22]. Halo TL, McMahon KM, Angeloni NL, Xu Y, Wang W, Chinen AB, Malin D, Strekalova E, Cryns VL, Cheng C, Mirkin CA, Thaxton CS, Proc. Natl. Acad. Sci. U. S. A 2014, 111, 17104. [PubMed: 25404304]

[23]. Chenab KK, Eivazzadeh-Keihan R, Maleki A, Pashazadeh-Panahi P, Hamblin MR, Mokhtarzadeh A, Nanomedicine 2019, 17, 342. [PubMed: 30826476]

[24]. He L, Lu DQ, Liang H, Xie S, Luo C, Hu M, Xu L, Zhang X, Tan W, ACS Nano 2017, 11, 4060. [PubMed: 28328200]

[25]. Riahi R, Wang S, Long M, Li N, Chiou PY, Zhang DD, Wong PK, ACS Nano 2014, 8, 3597. [PubMed: 24645754]

[26]. Wang S, Riahi R, Li N, Zhang DD, Wong PK, Adv. Mater 2015, 27, 6034. [PubMed: 26314800]

[27]. Tay CY, Yuan L, Leong DT, ACS Nano 2015, 9, 5609. [PubMed: 25906327]

[28]. Shin SW, Lee BS, Yang K, Amornkitbamrung L, Jang MS, Ku BM, Cho SW, Lee JH, Bae H, Oh BK, Ahn MJ, Lim YT, Um SH, Sci. Reports 2017 71 2017, 7, 1.

[29]. Dean ZS, Riahi R, Wong PK, Biomaterials 2015, 37, 156. [PubMed: 25453946]

[30]. Xu L, Gao Y, Kuang H, Liz-Marzán LM, Xu C, Angew. Chemie Int. Ed 2018, 57, 10544.

[31]. Acuna GP, Bucher M, Stein IH, Steinhauer C, Kuzyk A, Holzmeister P, Schreiber R, Moroz A, Stefani FD, Liedl T, Simmel FC, Tinnefeld P, ACS Nano 2012, 6, 3189. [PubMed: 22439823]

[32]. Wapinski OL, Vierbuchen T, Qu K, Lee QY, Chanda S, Fuentes DR, Giresi PG, Ng YH, Marro S, Neff NF, Drechsel D, Martynoga B, Castro DS, Webb AE, Südhof TC, Brunet A, Guillemot F, Chang HY, Wernig M, Cell 2013, 155, 621. [PubMed: 24243019]

[33]. Falagan-Lotsch P, Grzincic EM, Murphy CJ, Proc. Natl. Acad. Sci. U. S. A 2016, 113, 13318. [PubMed: 27821760]

[34]. Lobo MK, Karsten SL, Gray M, Geschwind DH, Yang XW, Nat. Neurosci 2006, 9, 443. [PubMed: 16491081]

[35]. Finegersh A, Homanics GE, J. Neurosci. Methods 2016, 263, 81. [PubMed: 26868730]

[36]. Martin D, Xu J, Porretta C, Nichols CD, ACS Chem. Neurosci 2017, 8, 356. [PubMed: 28135061]

[37]. Kishi Y, Gotoh Y, STAR Protoc 2021, 2, DOI 10.1016/J.XPRO.2021.100540.

[38]. Troshev D, Blokhin V, Ukrainskaya V, Kolacheva A, Ugrumov M, Front. Mol. Neurosci 2022, 15, 1020070. [PubMed: 36568278]

[39]. Holt LM, Stoyanof ST, Olsen ML, Curr. Protoc. Neurosci 2019, 88, e71. [PubMed: 31216394]

[40]. Welzel G, Seitz D, Schuster S, Sci. Reports 2015 51 2015, 5, 1.

[41]. Perez RA, Choi S-J, Han C-M, Kim J-J, Shim H, Leong KW, Kim H-W, Prog. Mater. Sci 2016, 82, 234.

[42]. Loo JFC, Ho HP, Kong SK, Wang TH, Ho YP, Adv. Biosyst 2019, 3, 1900138.

[43]. Wu C, Lillehoj PB, Wang P, Analyst 2015, 140, 7048. [PubMed: 26308143]

[44]. Grune T, Ott C, Häseli S, Höhn A, Jung T, Sci. Reports 2019 91 2019, 9, 1.

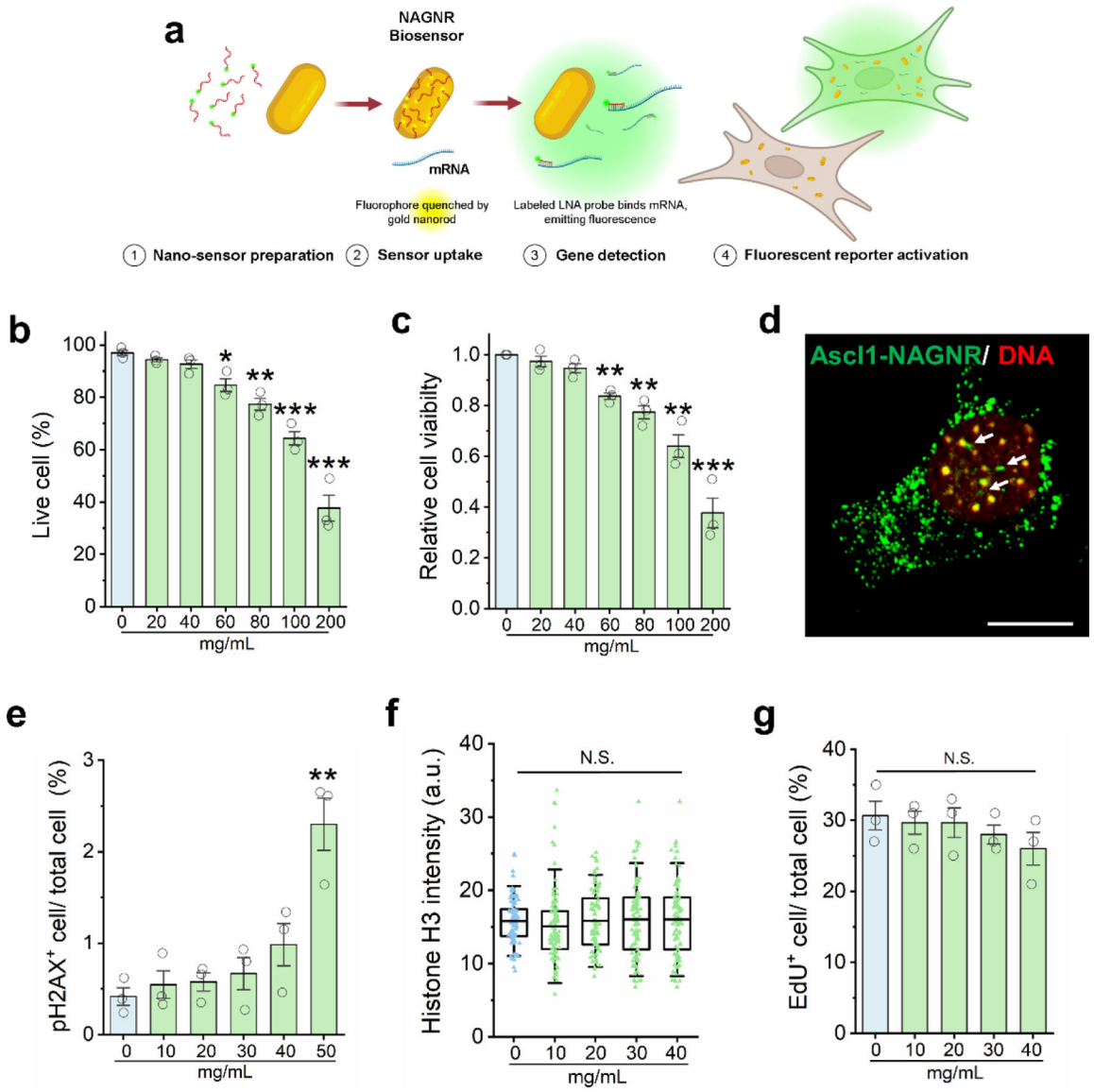

Figure 1. Biosafety assays of nucleic acid-based nanosensors using fibroblasts.

(a) Schematic diagram illustrating the design and workflow of nucleic acid-based gold nanorod (NAGNR) biosensors for cell sorting. **(b)** The percentage of live cells (Live/Dead staining) after incubating fibroblasts with different concentrations of gold nanorod biosensors for 6 hours and culturing for an additional 24 hours, as determined using a Live/Dead assay (n=3). **(c)** Cell viability of fibroblasts at 12 hours after incubation with different concentrations of gold nanorod biosensors for 6 hours, as determined by the PrestoBlue® cell viability assay. Cell viability was normalized to the control (the viability of cells not incubated with nanosensors) (n=3). **(d)** Immunofluorescent images show a BAM-transduced fibroblast expressing *Ascl1* mRNA after incubating with 40 μg/mL *Ascl1*-NAGNRs for 6 hours. White arrows indicate the presence of nanosensors in the cell nucleus. Scale bar, 10 μm. **(e)** The percentage of DNA damaged cells ($pH2AX^+$) after incubating fibroblasts with different concentrations of gold nanorod biosensors for 6 hours and culturing for an

additional 24 hours, as determined using the $pH2AX^+$ assay (n=3). **(f)** Histone H3 intensity was quantified from immunofluorescent images after incubating fibroblasts with different concentrations of gold nanorod biosensors for 6 hours and culturing for an additional 24 hours (n=100). **(g)** Quantification of cell proliferation (EdU^+) after incubating fibroblasts with different concentrations of gold nanorod biosensors for 6 hours and culturing for an additional 24 hours (n=3). In **b**, **c**, **e** and **g**, bar graphs show mean ± one standard deviation (SD). In **f**, box plot shows the ends at the quartiles, the mean as a horizontal line in the box, and the whiskers represent the SD. In **b**, **c**, **e-g**, statistical significance was determined by a one-way ANOVA and Tukey's multiple comparison test (NS: not significant, *p<0.05, **p<0.01, ***p<0.001).

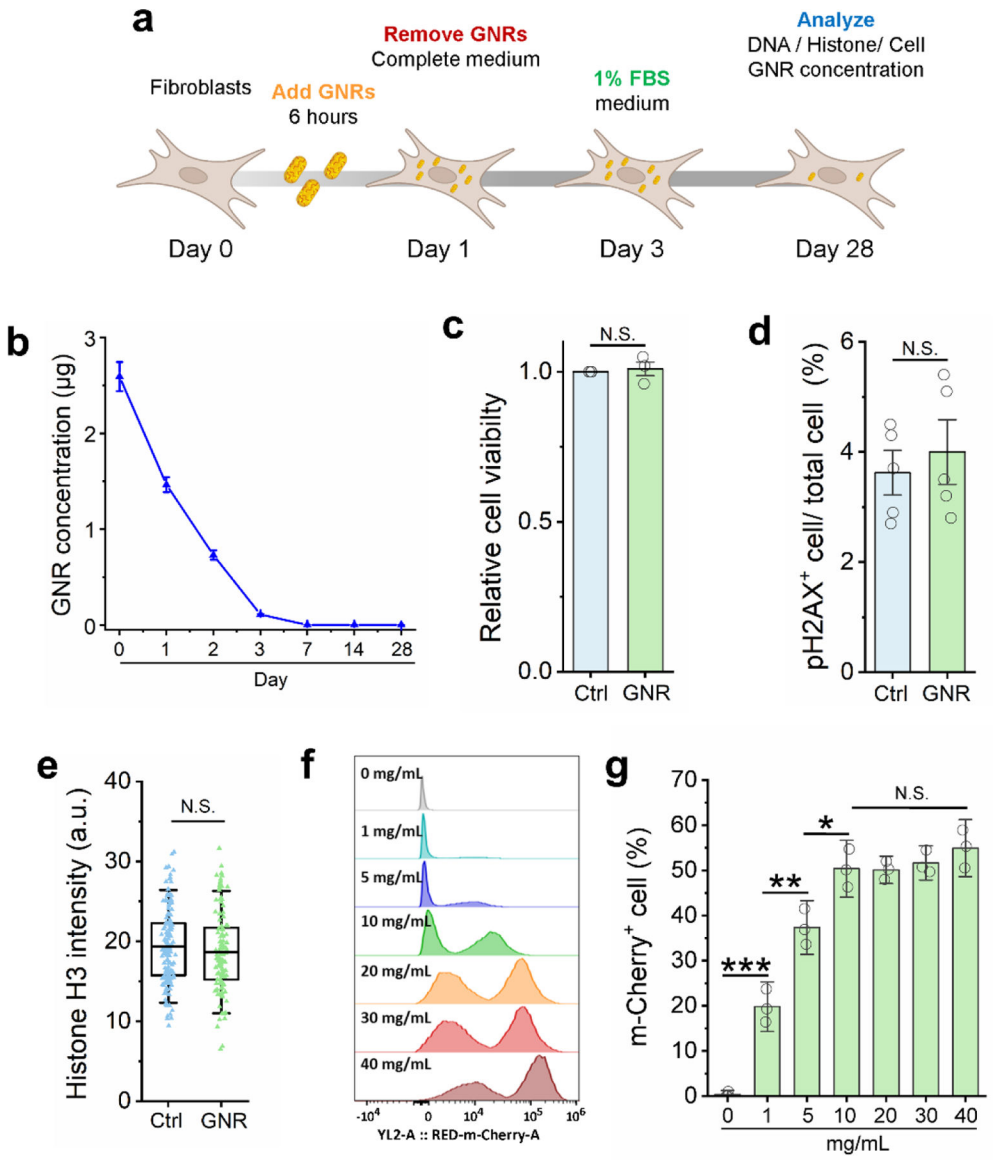

Figure 2. Long-term effect of nucleic acid-based nanosensors for cell sorting.

(a) Schematic diagram of the experimental timeline to determine the long-term effect of NAGN biosensors on fibroblasts. **(b)** The concentration of gold nanorods in cells at different time points after incubating fibroblasts with the biosensors for 6 hours, as determined by inductively coupled plasma mass spectrometry (n=3). **(c)** Cell viability of fibroblasts at 28 days after incubating fibroblasts with 40 μg/ml gold nanorods for first 6 hours, as determined by the PrestoBlue® cell viability assay. Cell viability was normalized with the control (the viability of cells not incubated with gold nanorods) (n=3). **(d)** The percentage of DNA damaged cells ($pH2AX^+$) at 28 days after incubating fibroblasts with 40 μg/ml gold nanorods for first 6 hours (n=5). **(e)** Histone H3 intensity was quantified from immunofluorescent images after incubating fibroblasts with the gold nanorods for first 6 hours and then culturing up to day 28 (n=100). **(f)** Flow cytometry was used to sort $mCherry^+$ fibroblasts from a population of fibroblasts incubated with

different concentrations of the *β-actin*-Alexa Fluor 546 NAGNR biosensors and mixed with non-treated fibroblasts at a 1:1 ratio. **(g)** The percentage of $mCherry^+$ cells sorted by FACS in **f** (n=3). In **b**, line graph shows mean ± SD. In **c**, **d**, and **g**, bar graphs show mean ± SD. In **e**, box plot shows the ends at the quartiles, the mean as a horizontal line in the box, and the whiskers represent the SD. In **c-e**, statistical significance was determined by a two-tailed, unpaired *t* test (NS: not significant). In **g**, statistical significance was determined by a one-way ANOVA and Tukey's multiple comparison test (NS: not significant, *p<0.05, **p<0.01, ***p<0.001).

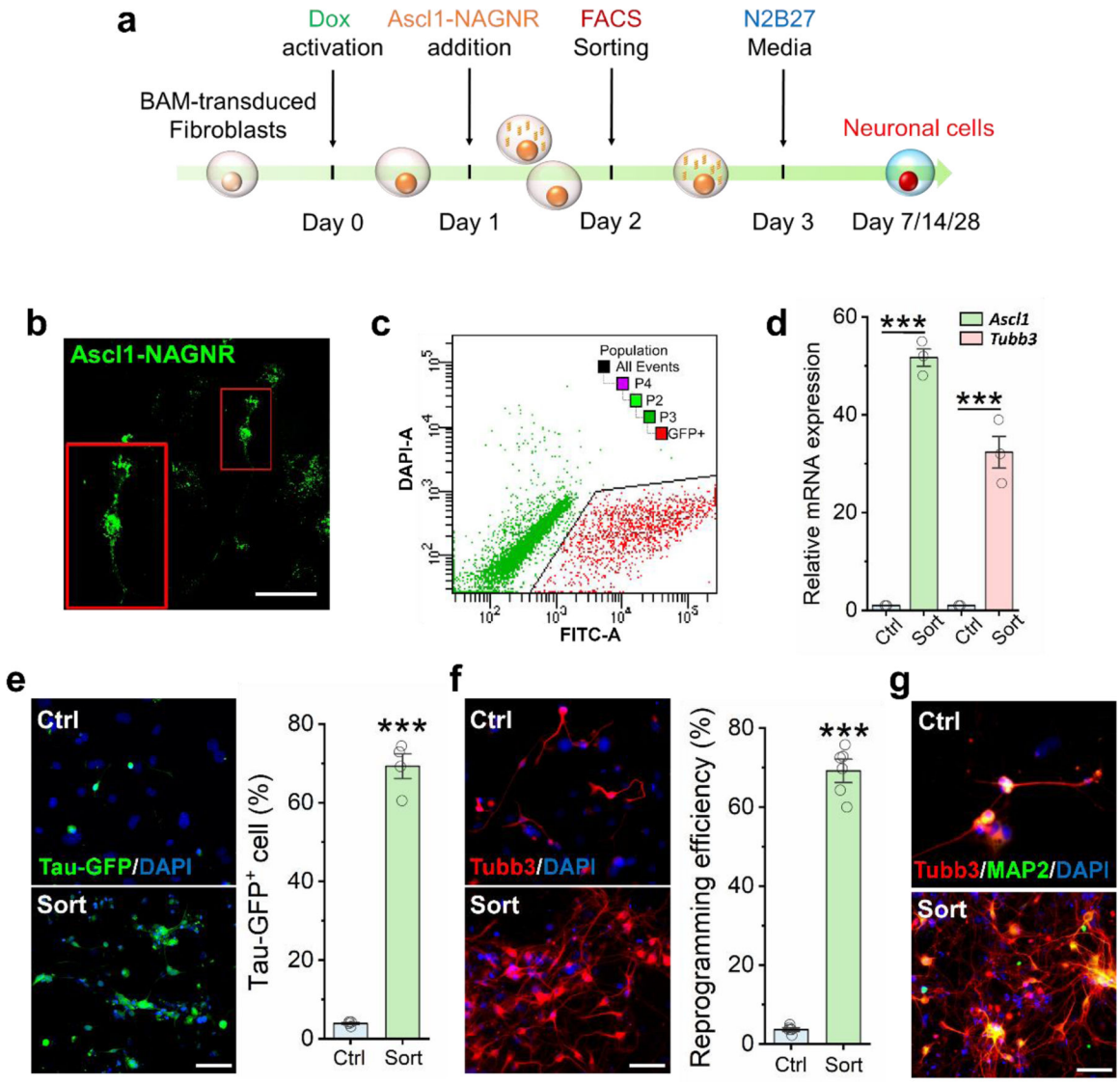

Figure 3. Sorting induced neuronal cells at the early stage of iN reprogramming using an Ascl1-NAGNR biosensor.

(a) Experimental timeline for culturing iN cells sorted using an Ascl1-NAGNR biosensor. **(b)** Immunofluorescent images show *Ascl1* mRNA expression in BAM-transduced fibroblasts incubated with the Ascl1-NAGNR biosensor for 6 hours, where the red outline provides a zoomed-in region highlighting Ascl-NAGNR^{+} cells. Scale bar, 100 μm. **(c)** FACS was used to sort Ascl1- ATTO488^{+} cells from Dox activated BAM-transduced fibroblasts on day 2 of the reprogramming process. **(d)** Relative *Ascl1* and *Tubb3* mRNA expression in control and sorted cells at day 1 and day 3, respectively, after sorting Dox activated BAM-transduced fibroblasts using an Ascl1-NAGNR biosensor (n=3). **(e)** BAM-transduced Tau-GFP fibroblasts were either sorted using an Ascl1-NAGNR biosensor or kept as a control (ctrl; i.e., not sorted) and cultured for 4 days. Immunofluorescent images show Tau-GFP^{+} cells at day 4, as quantified in the bar graph (n=4). Scale bar, 200 μm. **(f)** Reprogramming efficiency of BAM-transduced fibroblasts that were either sorted or not sorted. At day 7, the cells were fixed and stained for Tubb3, followed by immunofluorescence microscopy to

quantify Tubb3$^+$ iN cells (n=6). Scale bar, 200 μm. **(g)** Representative images of Tubb3$^+$ cells expressing mature neuronal marker MAP2 at 4 weeks after sorting. Scale bar, 200 μm. In **d**–**f**, bar graphs show mean ± SD. In **d**, statistical significance was determined by a one-way ANOVA and Tukey's multiple comparison test (***p<0.001). In **e-f**, statistical significance was determined by a two-tailed, unpaired *t* test (***p<0.001).

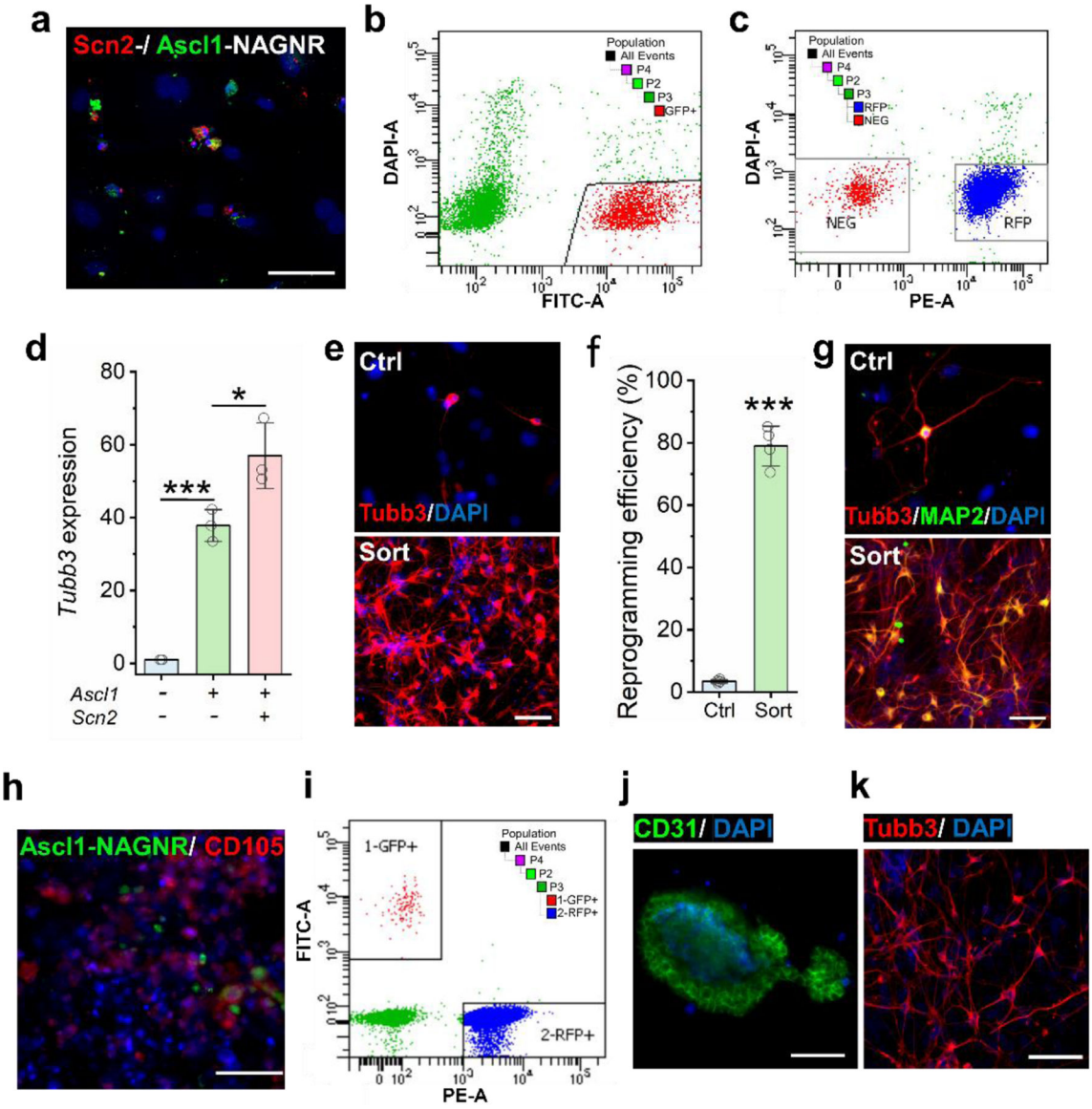

Figure 4. Sorting iN cells using multiple NAGNR biosensors and in conjunction with protein-based cell sorting.

(a) Representative immunofluorescent images show that a Scn2-Alexa Fluor 546 NAGNR biosensor can detect *Scn2* mRNA expression in Ascl1-NAGNR biosensor sorted cells (Ascl1$^+$). Scale bar, 100 μm. **(b)** FACS was used to sort Ascl1-ATTO488$^+$ cells from Dox activated BAM-transduced fibroblasts. **(c)** FACS was used to sort Scn2-AlexaFluor 546$^+$ cells from Ascl1-ATTO488$^+$ cells one day after sorting cells using an Ascl1-NAGNR biosensor. **(d)** Relative *Tubb3* mRNA expression in Ascl1-NAGNR sorted cells, Ascl1-NAGNR + Scn2-NANGR sorted cells and control cells (not sorted) at day 3 (n=3). **(e)** Representative images of Tubb3$^+$ iN cells at day 7 that were sorted with Ascl1-NAGNR + Scn2-NAGNR biosensors. Scale bar, 200 μm. **(f)** Reprogramming efficiency of BAM-transduced fibroblasts that were sorted by Ascl1-NAGNR + Scn2-NAGNR biosensors (n=6). On day 7, the cells were fixed and stained for Tubb3, followed by immunofluorescence microscopy to quantify Tubb3$^+$ iN cells. **(g)** Representative images of Tubb3$^+$ cells

expressing mature neuronal marker MAP2 at 4 weeks after sorting. Scale bar, 200 μm. **(h)** Representative immunofluorescent images show *Ascl1* mRNA and CD105 expression in mouse embryonic stem cells (mESCs) cultured with neuronal and endothelial media (1:1 ratio) for 10 days. *Ascl1* mRNA was detected using the Ascl1-ATTO488 NAGNR biosensor whereas CD105-RFP antibody was utilized to identify $CD105^+$ endothelial cells. Scale bar, 100 μm. **(i)** FACS was utilized to sort Ascl1-$ATTO488^+$ and $CD105\text{-}RFP^+$ cells from mESCs at day 10. **(j)** Representative immunofluorescent images show endothelial marker, CD31, expression at day 10 after sorting for $CD105\text{-}RFP^+$ cells from the mESC culture. Scale bar, 100 μm. **(k)** Representative immunofluorescent images show $Tubb3^+$ cells at day 7 after sorting for Ascl1-$ATTO488^+$ cells from the mESC culture. Scale bar, 100 μm. In **d** and **f**, bar graphs show mean ± SD. In **d**, statistical significance was determined by a one-way ANOVA and Tukey's multiple comparison test (*$p<0.05$, ***$p<0.001$). In **f**, statistical significance was determined by a two-tailed, unpaired *t* test (***$p<0.001$).

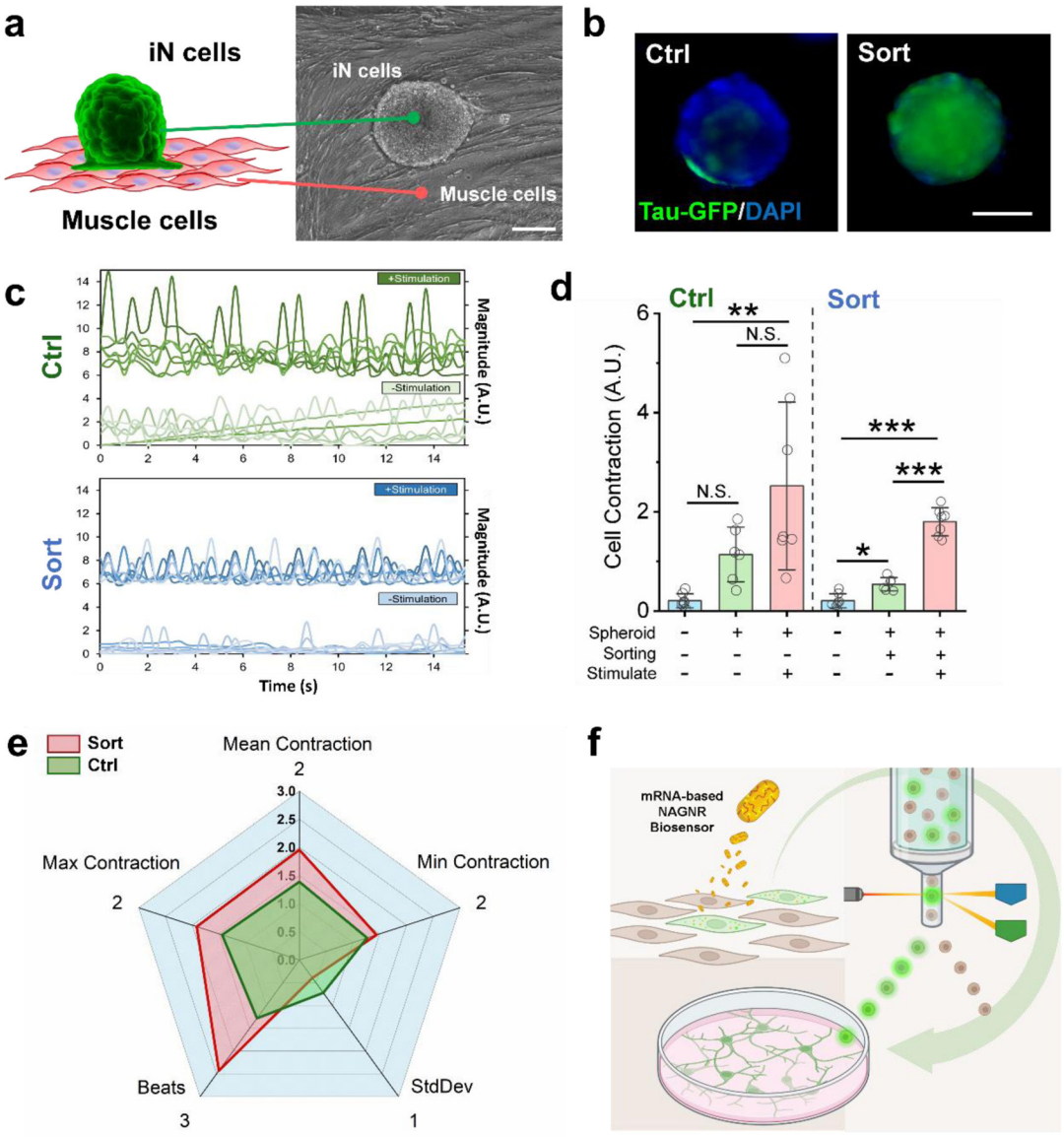

Figure 5. NAGNR-sorted induced neuronal cells are functional in a co-culture system.

(a) Schematic diagram of a neuromuscular junction *in vitro* model. Representative brightfield image show iN spheroid seeded on a monolayer of C2C12 cells. Scale bar, 100 μm. **(b)** Representative immunofluorescent images show Tau-GFP expression in sorted and non-sorted iN cell spheroids at day 4 after sorting cells using Scn2-NAGNR biosensors. Scale bar, 200 μm. **(c)** The waveform of C2C12 muscle cell contraction at day 10 after sorted and non-sorted iN spheroids were seeded on C2C12 and treated with 15 V electronic stimulation. **(d)** Quantification of cell contraction from non-sorted and sorted iN spheroids seeded on C2C12 cells and treated with or without 15 mV electronic stimulation (n=6). **(e)** Spider chart showing fold changes in average contraction parameters for control or sorted groups. Numerical values indicate the average parameter value of stimulated conditions normalized to that of non-stimulated (n=3). Each vertex indicates the average normalized value for maximum, mean, and minimum contraction, contraction standard deviation, or

number of beats. **(f)** Schematic diagram illustrating the potential utilization of NAGNR biosensors to label and sort cells based on mRNA expression for biomedical applications. In **d**, bar graphs show mean ± SD and statistical significance was determined by a one-way ANOVA and Tukey's multiple comparison test (NS: not significant, *p<0.05, ***p<0.001).